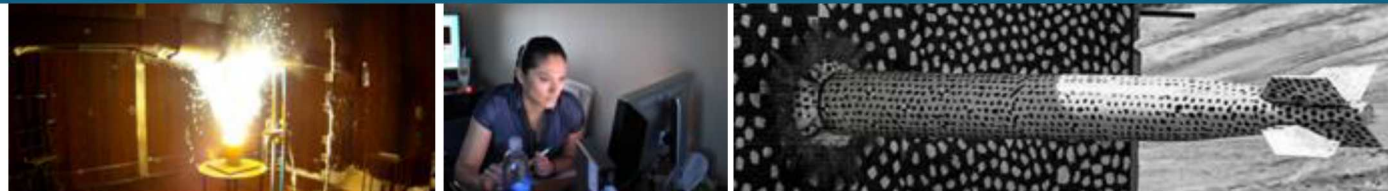




Sandia
National
Laboratories

SAND2020-10346C

A06-1066: *Operando Microcalorimetry Study on Irreversible Losses in Silicon Anodes*



ECS PRiME 2020 – Virtual Meeting

Prepared by

Eric Allcorn, Teal Harbour, David Arnot, Jill Langendorf, Linda Johnson



Sandia National Laboratories is a multimission laboratory managed and operated by National Technology & Engineering Solutions of Sandia, LLC, a wholly owned subsidiary of Honeywell International Inc., for the U.S. Department of Energy's National Nuclear Security Administration under contract DE-NA0003525.



- Materials and Methods
- Supporting Characterization
 - Cycle life, HPPC, dE/dT
- Microcalorimetry Data
 - Resulting curves, normalized heat flow
 - Impact of cycling voltage and cycling rate

Silicon Electrodes Studied



The electrodes studied here are from the ANL CAMP Electrode Library (A018) and are composed of:

- 80 wt. % active nSi: ~150nm from Paraclete Energy
- 10 wt. % Timcal C45 carbon black
- 10 wt. % LiPAA binder



Sourcing from CAMP library ensures consistency of electrodes, which is critical for experimental approach of *operando* Microcalorimetry (see Slide 7)

Electrode thickness	Total Areal Loading	Silicon Areal Loading	Areal Capacity (@ 50mV)
10 μm	1.10 mg/cm^2	0.88 mg/cm^2	1.74 mAh/cm^2

Microcalorimetry Background (I of 3)



Operando Microcalorimetry involves active electrochemical cycling of batteries inside of an isothermal microcalorimeter, allowing for real-time measurement of heat generated by the battery while cycling.

The measured heat flow comes from three general sources

- Ohmic heat – from current flow through a “resistor”
- Entropic heat – contribution from reversible lithiation reactions
- **Parasitic heat** – remainder of heat flow, primarily attributed to SEI



TAM IV Microcalorimeter

What we care about

- Lack of effective surface passivation is one of the primary causes of silicon anode capacity loss
 - The other is mechanical degradation from volume change during lithiation / delithiation
- Parasitic heat can serve as a battery scale characterization tool for the degree of silicon passivation (or lack thereof)

Microcalorimetry Background (2 of 3)



There are two approaches for isolation and determination of the parasitic heat flow from the total measured heat flow

1. Integrate total heat flow over a full charge-discharge cycle. Entropic heat is reversible so cancels out. Polarization heat can be determined from integrating the voltage curve hysteresis. Parasitic reaction is all that remains.
 - Upsides: Simplified testing / data processing
 - Downsides: No resolution beyond full cycles; only valid for cycles with low coulombic losses

$$Q_p = \left[\int_0^{t_d} \frac{dQ_d}{dt} dt + \int_0^{t_c} \frac{dQ_c}{dt} dt \right] - \left[\int_0^{t_c} I_c V_c dt - \int_0^{t_d} I_d V_d dt \right]$$

Reversible Heat - if discharge and charge capacities are roughly equal (high CE), the reversible portion of these terms are equal but opposite, so sum to zero

Ohmic Heat - if discharge and charge times are roughly equal (high CE) subtracting yields total polarization over full cycle, multiplied by current gives heat

Early cycle CE is too low in Si for this approach, may be viable for later cycles / more stable electrodes.

Microcalorimetry Background (3 of 3)



There are two approaches for isolation and determination of the parasitic heat flow from the total measured heat flow

1. Independently measure equilibrium potential and entropy effects in separate, but similar, cells. Use those values to calculate the polarization and entropic heat flow contributions at discrete points of charge / discharge. Fit a curve and subtract from total heat flow to determine parasitic reactions.
 - Upsides: Can tolerate coulombic losses; provides detail at different points of charge / discharge
 - Downsides: More complex testing / data analysis; requires repeatable cell production for supporting tests

$$\dot{Q} = I(E_{\text{load}} - E_{\text{eq}}) + IT\left(\frac{dE_{\text{eq}}}{dT}\right) + \dot{Q}_p$$



Ohmic Heat, also
representable as
 I^2R_{int}



Reversible heat

This is the approach utilized
in this work.

Testing Approach



Operando Microcal protocol:

- Cycle number: 10
- Rate: C/10 **or** C/15 **Study effect of cycle rate**
- Voltage: 0.05 – 1.5V **or** 0.10 – 1.5V
Study effect of lower voltage cutoff

CR2032 - half cells

Active:	80% nano-Si
Counter:	Lithium foil
Electrolyte	1.2M LiPF ₆ in EC:EMC
Elyte Vol.	120 μ L per cell

Supporting analysis

- Internal Resistance Analysis
 - HPPC or EIS as a function of %SOC on select cycles
 - Supports determination of ohmic heat contribution
- Entropy Contribution
 - OCV vs Temperature as a function of %SOC on select cycles
 - Supports determination of reversible heat contribution
- Cycle Life Testing
 - 100 cycle test protocol to enable correlation of microcal results with cycle life

A single *operando* Microcalorimetry test requires two supporting tests for determination of parasitic heat, and one additional test for correlation with cycle life

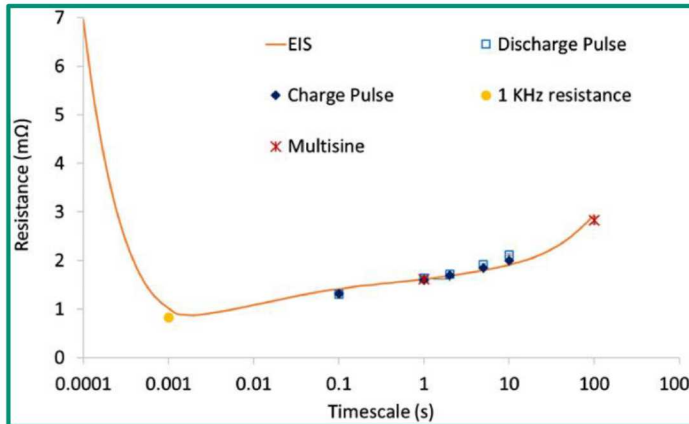
Test Protocols for R-internal

$$\dot{Q}_{ohmic} = I\eta = I(E_{load} - E_{eq}) = R_{int}I^2$$

E_{eq} used for microcal fit curves. R-int enables visualization of cell evolution with %SOC and cycle number

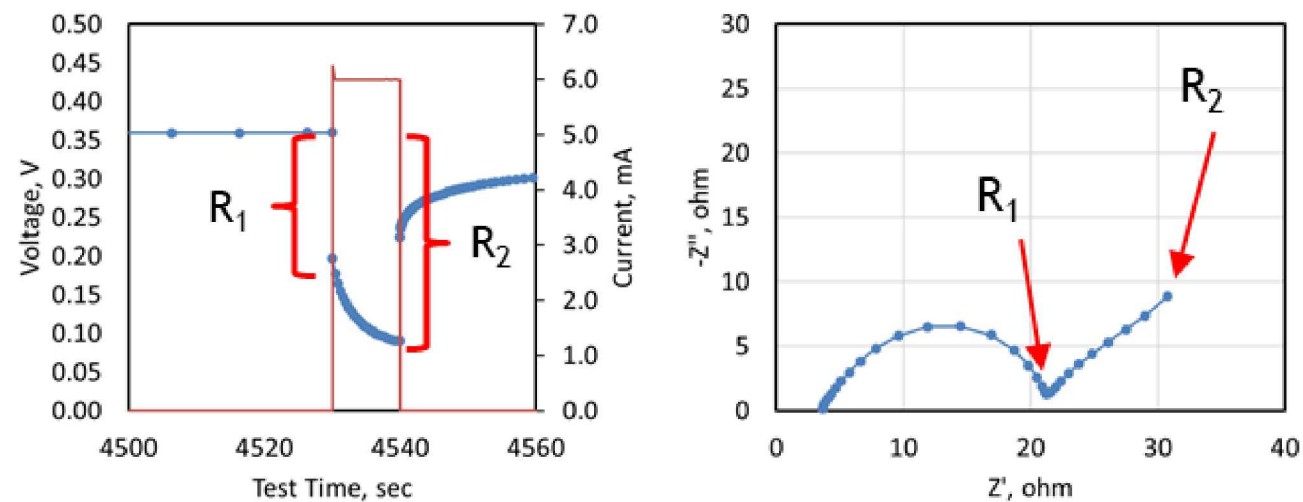
Three protocols tested for measuring E_{eq} and R-int at various states-of-charge during cycling

- HPPC1: HPPC conducted every 12 minutes (~ 50 per cycle) for increased data resolution
 - Longer cycling and more HPPC may impact results
- HPPC2: HPPC conducted every hour (~ 10 per cycle) for faster cycling and reduced impact
 - Lower resolution if R-int varies significantly
- EIS1: EIS conducted every half hour as a secondary method to confirm HPPC values
 - Limited channels for analysis



A. Barai et. al. *Progress in Energy and Combustion Science* 72 (2019) 1-13.

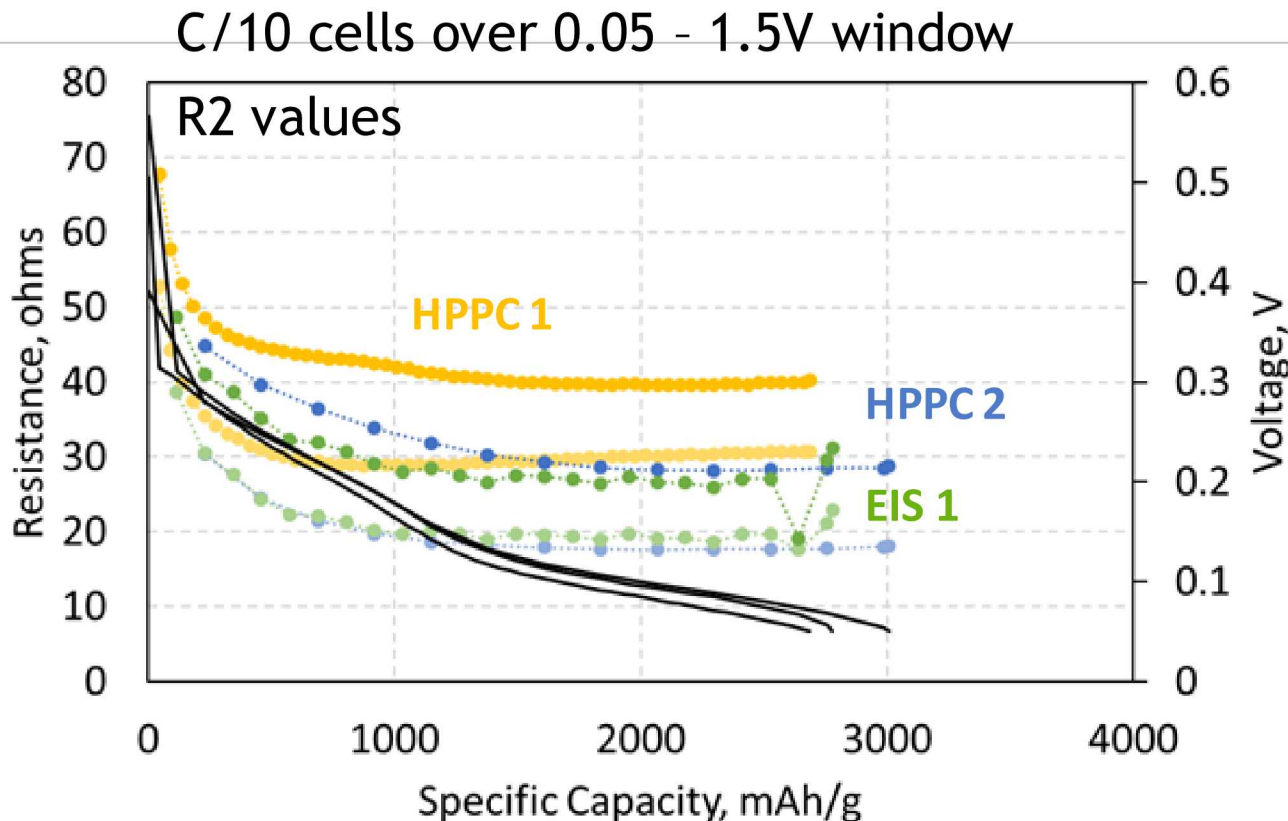
Similar timescales of analysis yield similar results across methods



Two R-int values determined for each data point

- R1 instantaneous, ~ 0.1 s timescale
- R2 diffusional, ~ 10 s timescale

R-internal Comparison Across Methods



- Relatively constant R-int values, with exception of low SOC on charge, means low resolution testing is acceptable
- Delivered capacity and voltage curves are similar
 - Slightly lower voltage, less capacity for HPPC1 cell
- Close agreement in R-int for HPPC2 and EIS
 - HPPC1 measures an appreciably higher R-int value

High number of pulses and/or extended cycle time for HPPC1 protocol results in greater resistance / more SEI than under typical cycling conditions

HPPC2 protocol is employed. Delivers more accurate results than HPPC1 and easier to implement than EIS

Internal Resistance as a Function of %SOC and Cycle

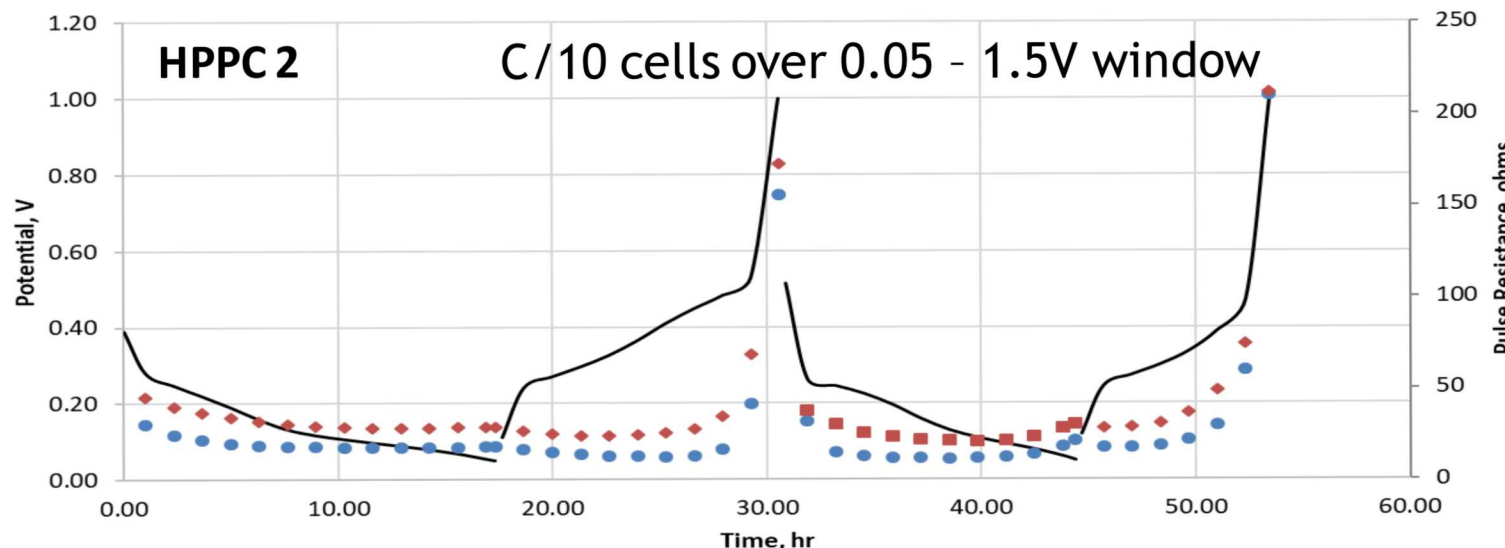


HPPC2 results of measured R-int over the first 2 cycles

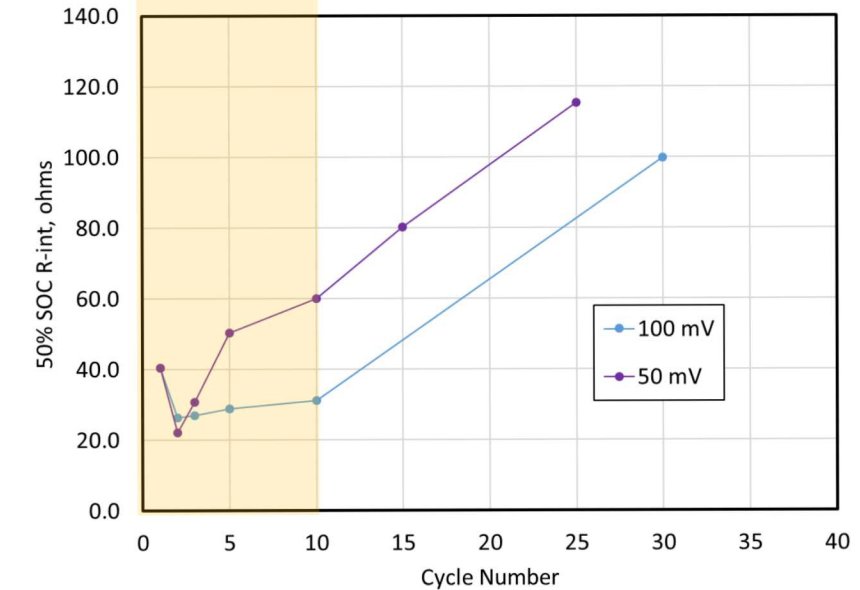
- Relatively constant, except for low %SOC conditions, especially during charge
- R1 is consistently lower than R2

R-int at 50%SOC as a function of cycle for two different lower voltage cutoffs: 100mV and 50mV

- Very similar in first few cycles, but resistance in 50mV cell grows much faster than for 100mV cell



Window of Microcal Analysis



— Voltage
● R1
● R2

E_{eq} values from HPPC2 used for determination and subtraction of ohmic heat from *operando* microcal analysis

Q-rev Determination, Methods to Measure dE_{eq}/dT

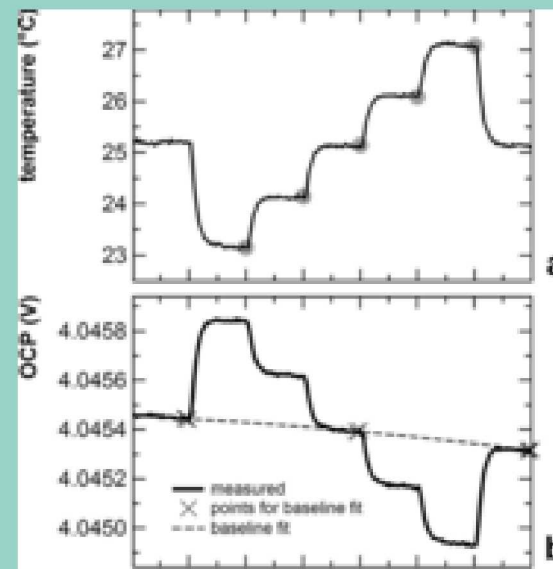


$$\dot{Q}_{rev} = \frac{T}{nF} \Delta S = TI \frac{dE}{dT}$$

Derivation in literature
(Housel et.al.) if more detail is desired

Need to experimentally determine dE_{eq}/dT at various states of charge

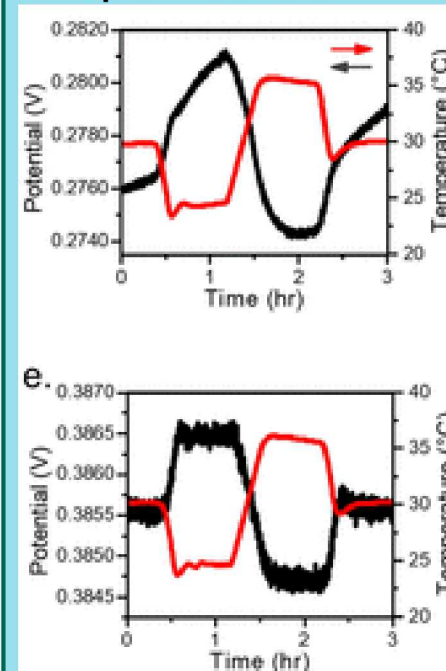
Step Method



$\Delta V/\Delta T$ based on averaging across multiple temperature steps

a. Typically includes positive and negative deviations to allow for a baseline voltage determination

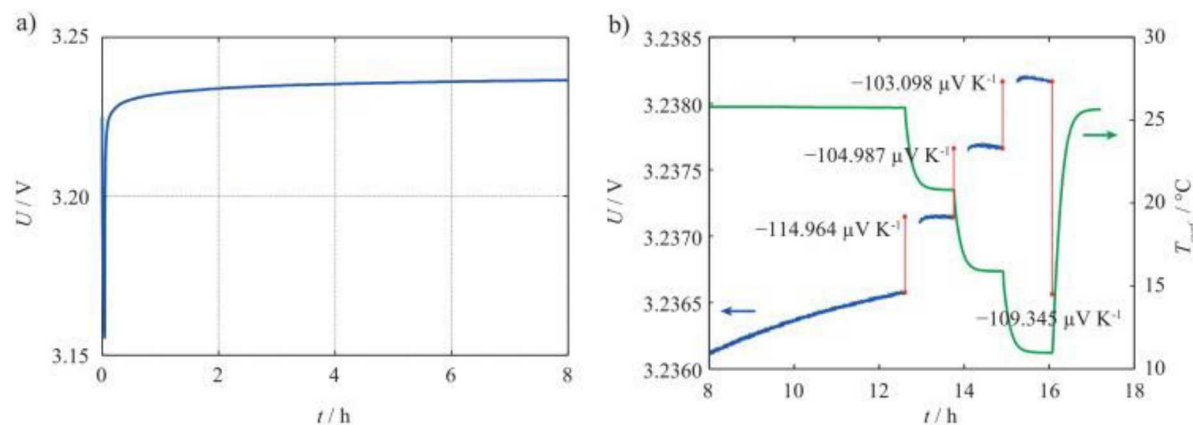
Slope Method



$\Delta V/\Delta t$ and $\Delta T/\Delta t$ slopes both determined to yield a $\Delta V/\Delta T$ value

Fewer datapoints to generate a confident average but potentially less susceptible to drifting baselines

Challenges of Step Method



J P Schmidt, A. Weber, E. Ivers-Tiffey. *Electrochimica Acta* 137 (2014) 311-319.

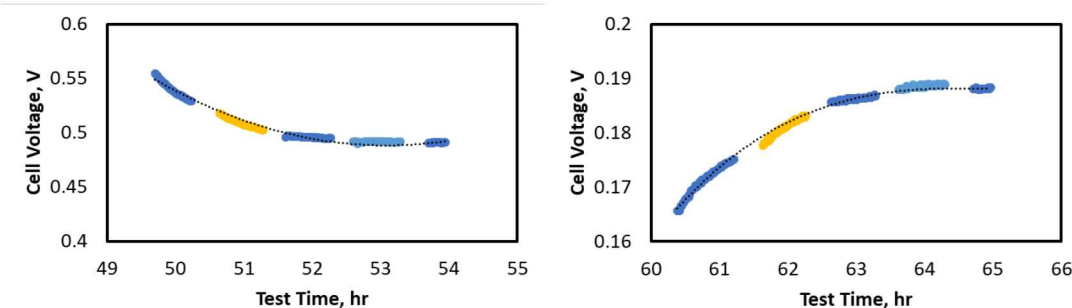
Requires a stable OCV for accurate determination of voltage delta across temperature steps

Literature shows appreciable continued drift even after 8 hours of rest, not feasible using multiple steps per cycle so we employed 1 hour OCVs and attempted to fit a baseline

Silicon is non-passivated, so OCV drift is expected due to %SOC shifts. This further impedes the determination of a stable OCV

Determination of voltage delta requires applying a fit curve to baseline temperature voltage

- With strong OCV drift the fitting parameters play a significant role in delta V values

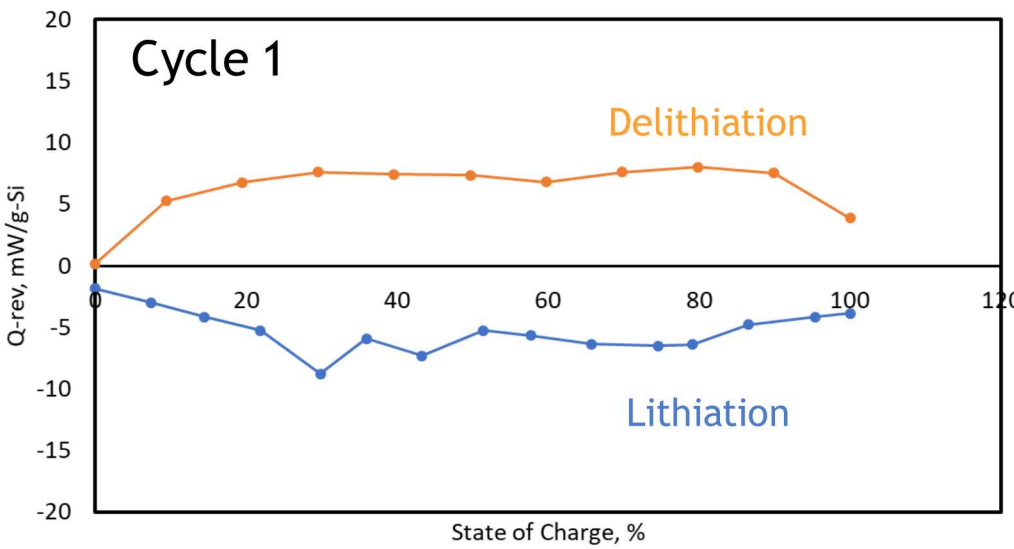


Slow OCV stabilization and drifting silicon OCV resulted in poor results for Step Method, so this approach was not used for *operando* microcal correction

Q-rev as a Function of %SOC Using Slope Method



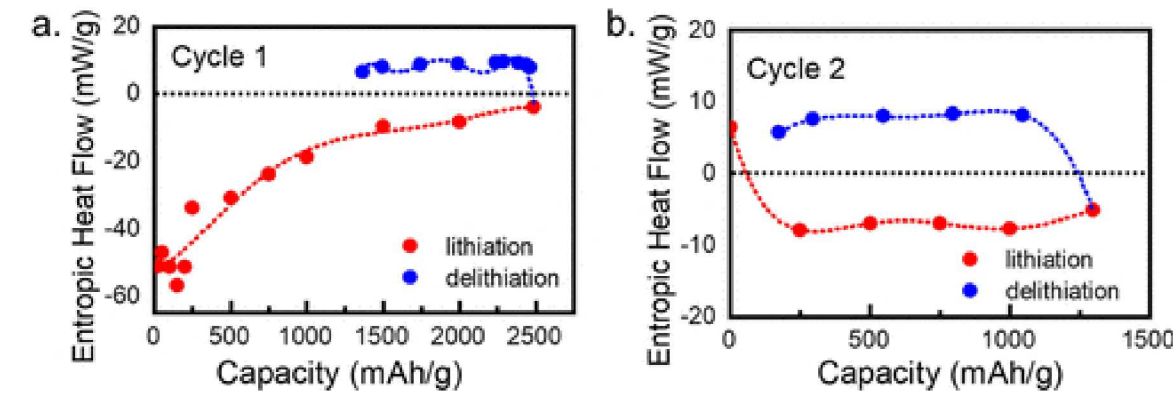
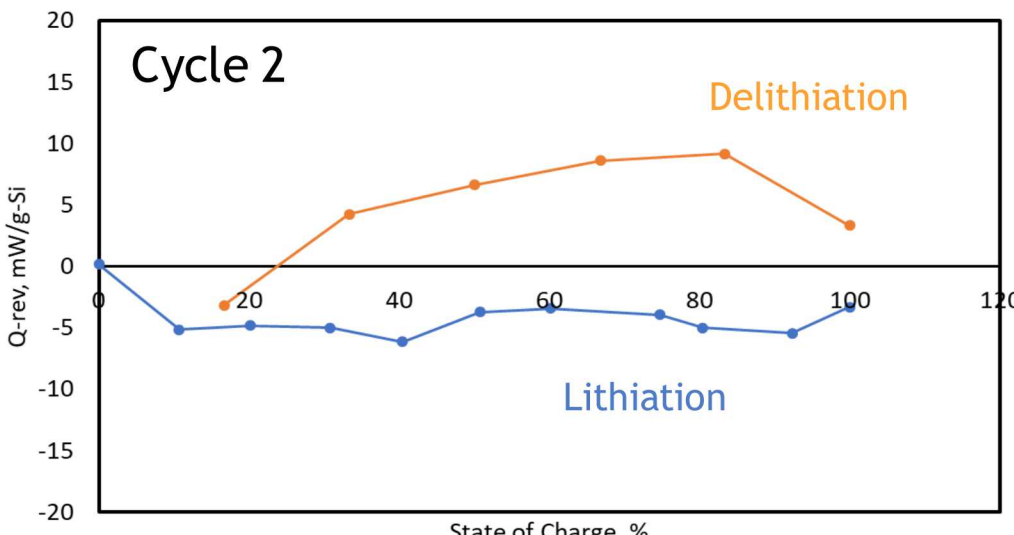
C/10 cells over 0.05 - 1.5V window



Slope method delivers strong agreement of calculated reversible heat flow with literature

Differences observed in initial lithiation values are likely associated with differences in the crystallinity of starting silicon materials

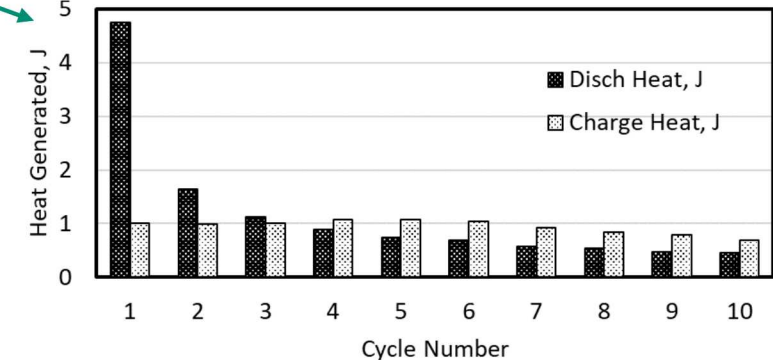
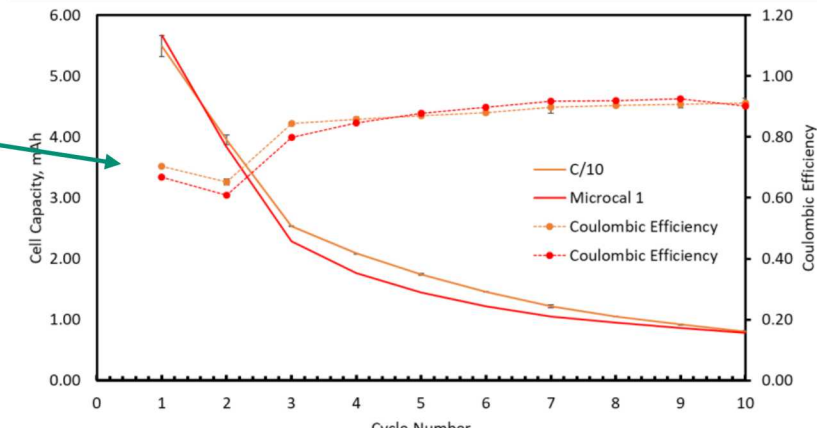
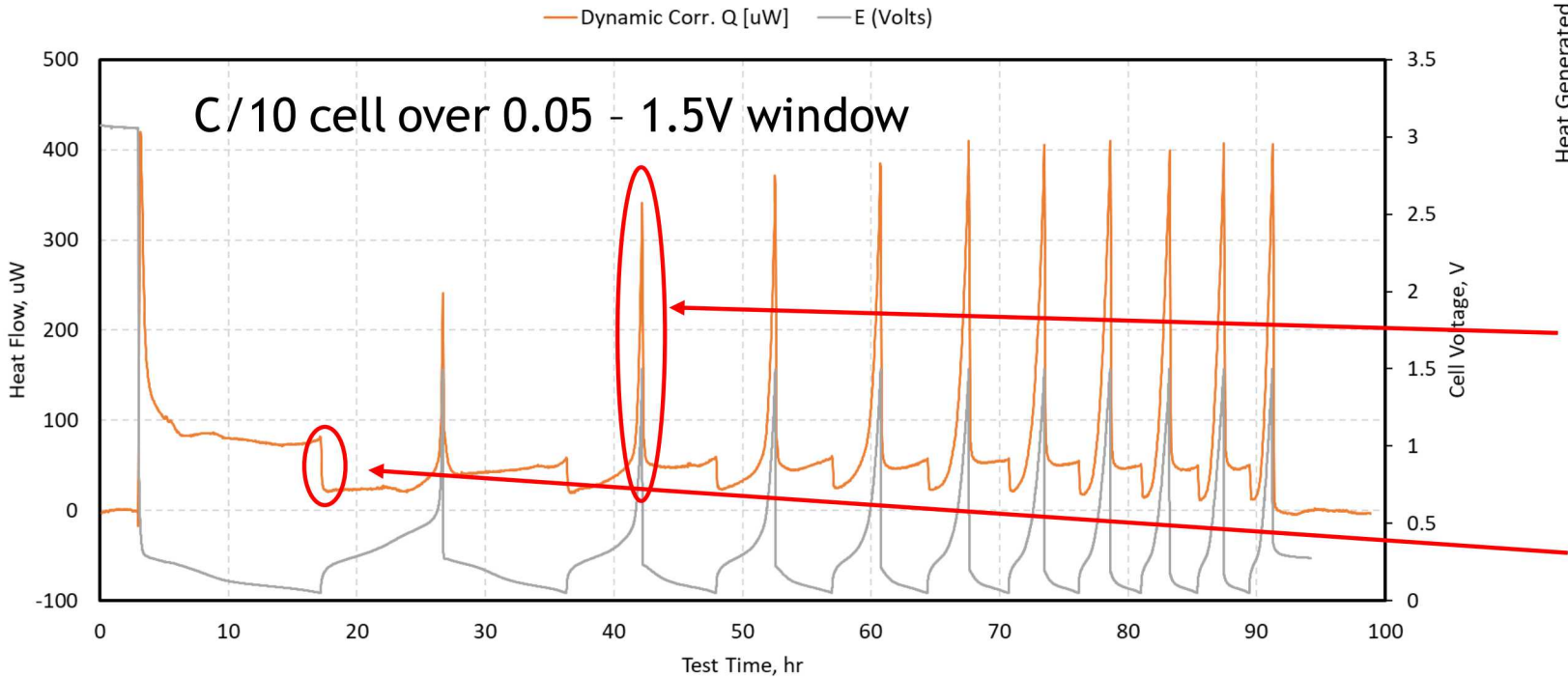
dE_{eq}/dT values from the Slope Method are used for determination and subtraction of Q-rev from *operando* microcal analysis



Operando Microcalorimetry Total Heat Flow



- Strong agreement in electrochemical performance between *operando* cells and separately tested cycle-life cells
 - Validates approach of supporting tests to correct heat flow
- Most heat flow occurs in initial lithiation, gradual decay in heat generation with cycling
 - Some distortion from reduced capacity / cycling time in later cycles



Peak in heat flow at low %SOC, correlates to R-int spike measured previously

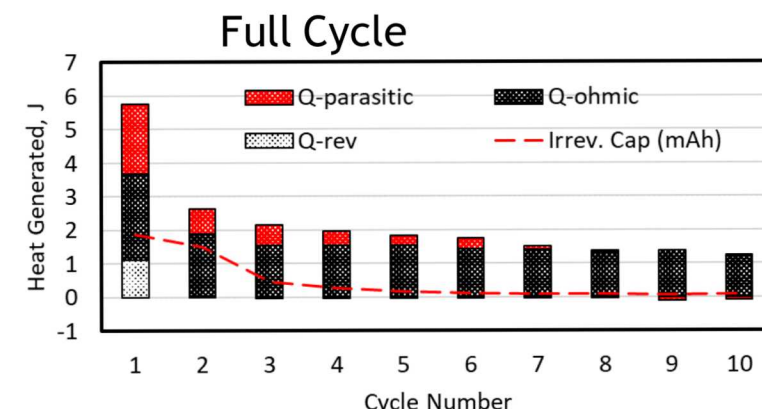
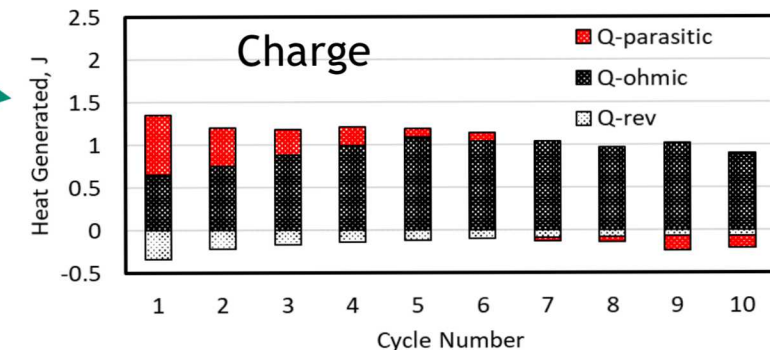
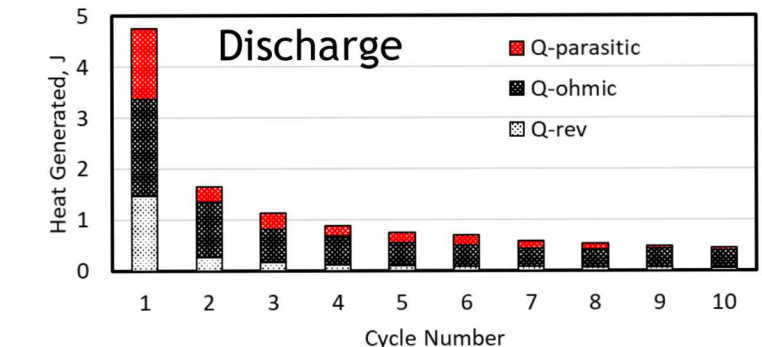
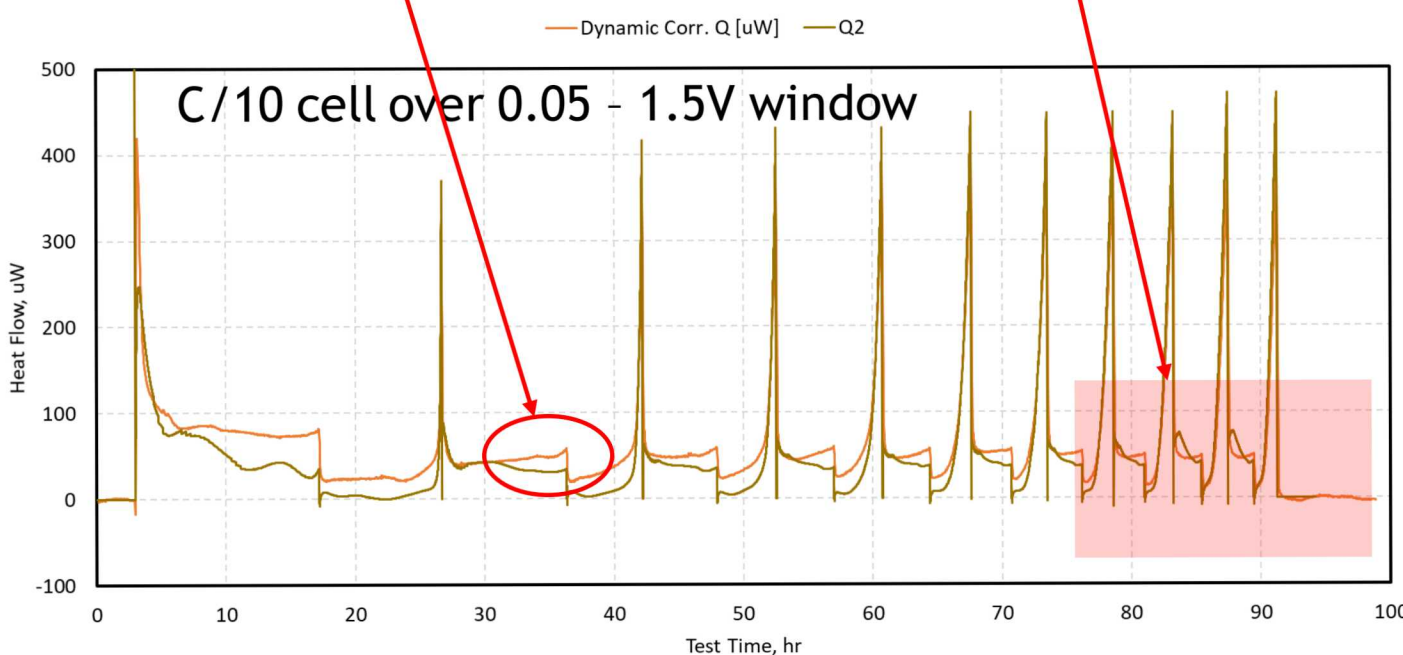
Steps in heat flow from charge / discharge as Q-rev signal goes from positive to negative

Relative Heat Flow Sources and Parasitic Contribution



Combination of previously determined ohmic and reversible contributions shows close alignment with measured total heat flow, with clear deviations that are attributed to parasitic heat flow

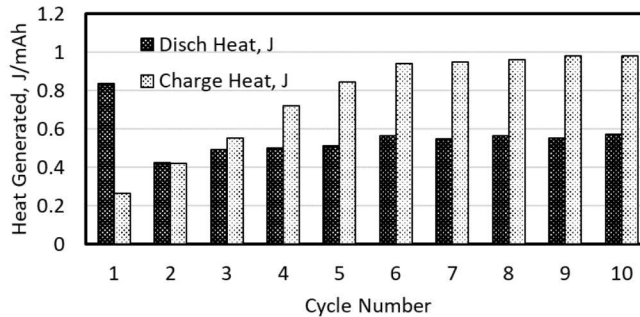
- This parasitic heat flow is strongest at high SOC
- Capacity loss results in poorer quality fit curves and questionable parasitic data for later cycles
- Integration over full cycles enables quantification and comparison of sources



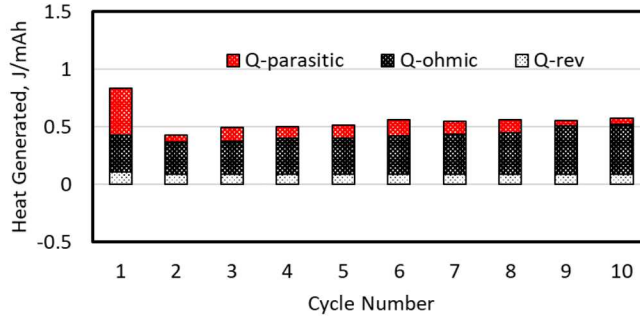
Heat Flow Breakdown: Baseline C/10 Cell over 0.05 – 1.5V



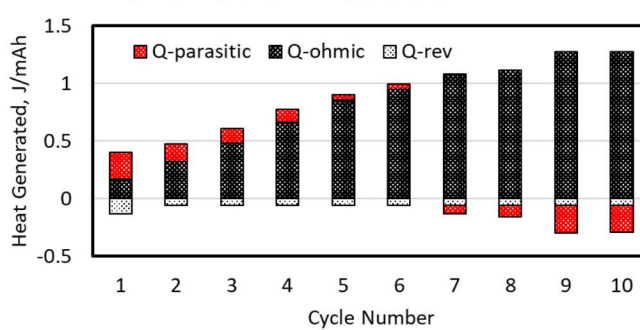
Normalized Heat Gen.



Lithiation Heat Gen.



Delithiation Heat Gen.



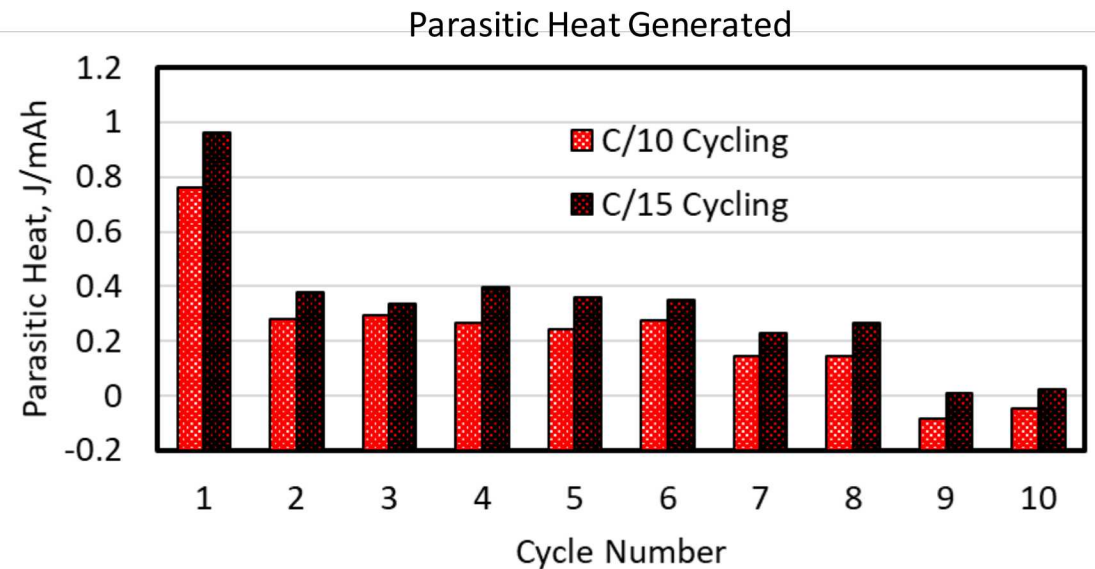
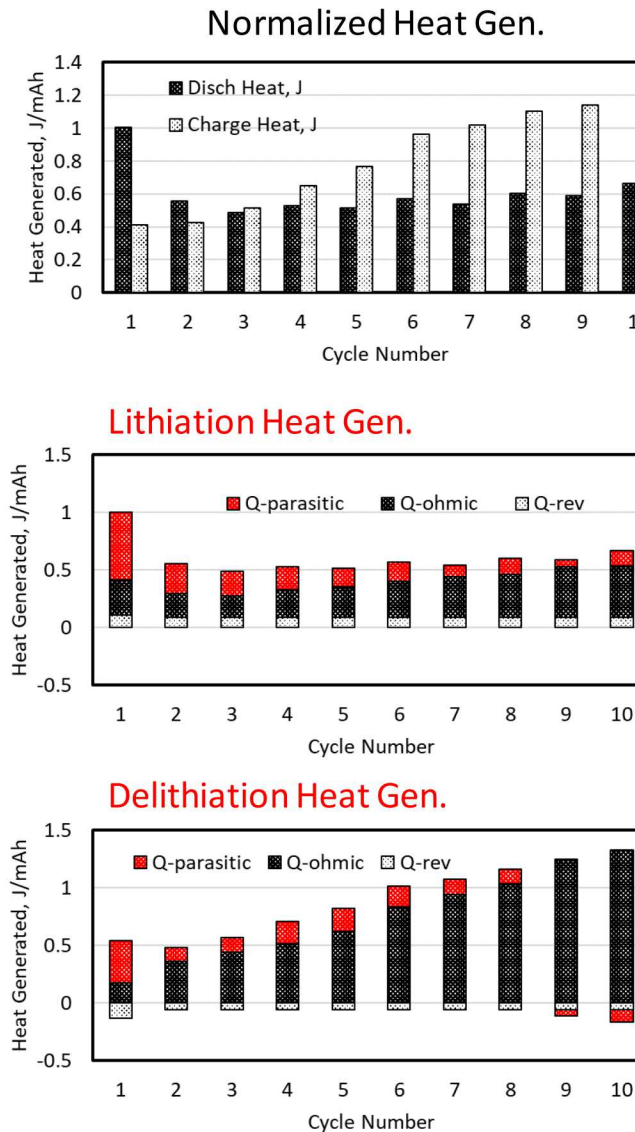
Heat Generation is Normalized to Capacity per Cycle

- More consistent heat flow per cycle, more persistent parasitic flow, and accounts for fading of cells

Overall trends point to early losses from SEI growth / passivation, later losses from impedance growth / material pulverization

- High parasitic heat during initial lithiation, stable in subsequent cycles
- Dramatically increasing delithiation heat primarily arising from ohmic heat flow
 - Indicates failure arising from impedance effects; i.e. active material pulverization or SEI blocking
- Later cycles (>7) still show questionable results likely from poor quality fit curves after capacity decay

Impact of Cycle Rate: C/15 Cell over 0.5 – 1.5V

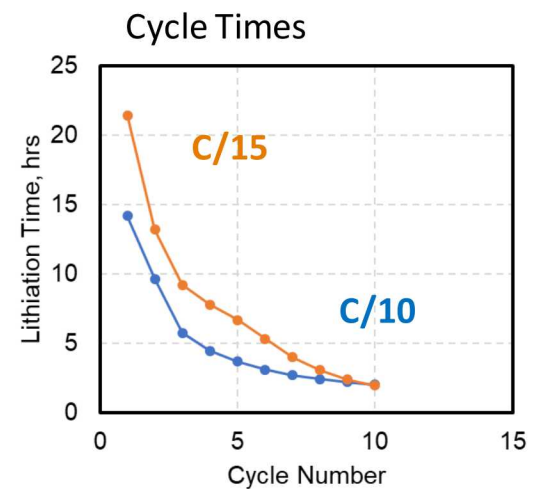


Overall trends appear to closely match C/10 cell with same voltage window

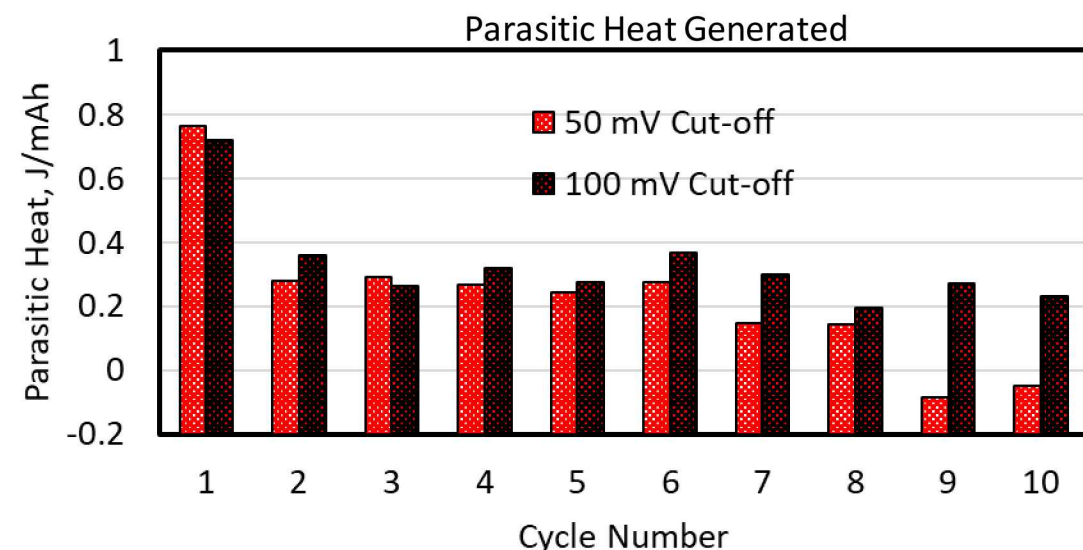
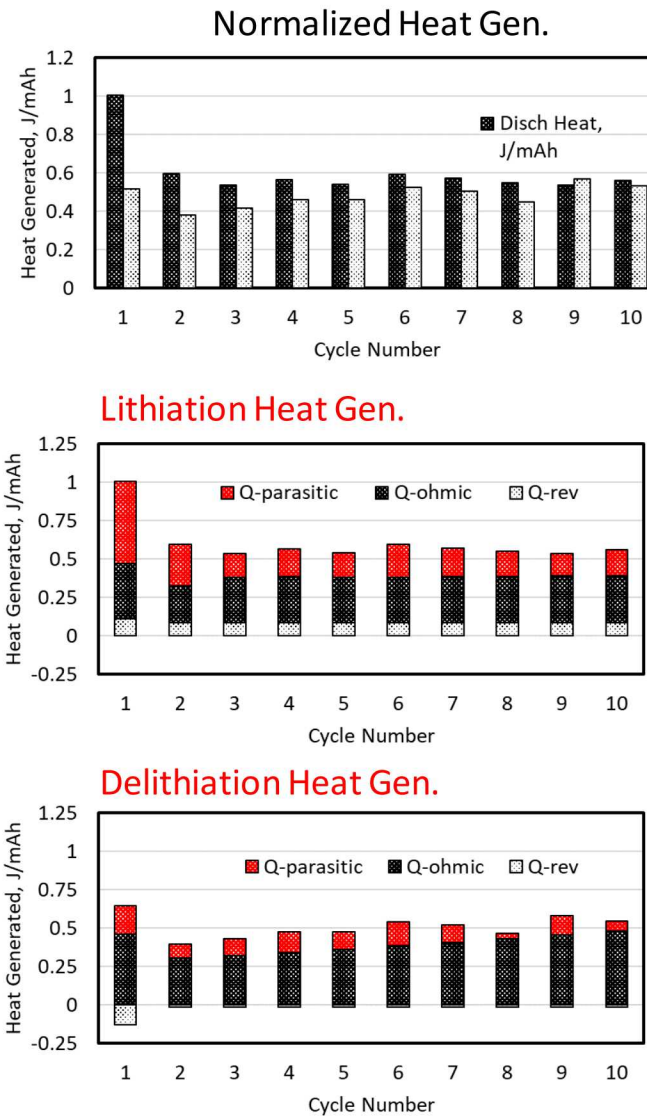
- Stable normalized heat flow during lithiation
- Increasing ohmic heat flow during delithiation

Similar electrochemical performance between cells

Longer cycling times from lower C-rate translate to consistently higher normalized parasitic heat flow. SEI is not fully passivating and has a time dependency



Impact of Voltage Cut-off: C/10 Cell over 0.10 – 1.5V



Higher cut-off 100 mV cell shows much more stable electrochemical cycling (see slide 20 for more detail)

Heat flow behavior is quite different from 50mV cell in some respects

- No dramatic increase of ohmic heat flow, no impedance / pulverization failure

But very similar in others

- Total parasitic heat flow is approximately the same as for the 50mV cell, until later cycles when 50 mV cell is failing

Poor electrochemical results in 50mV cells do not appear to be a function of parasitic heat

Reaction Heat from Lost Capacity

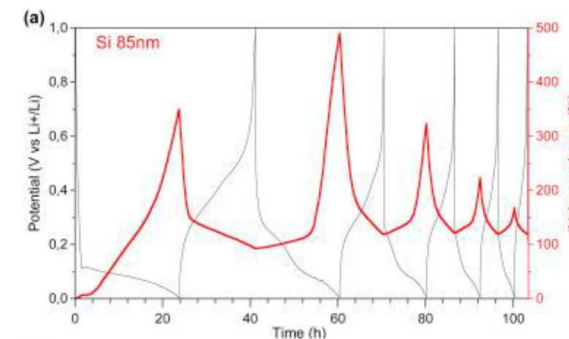
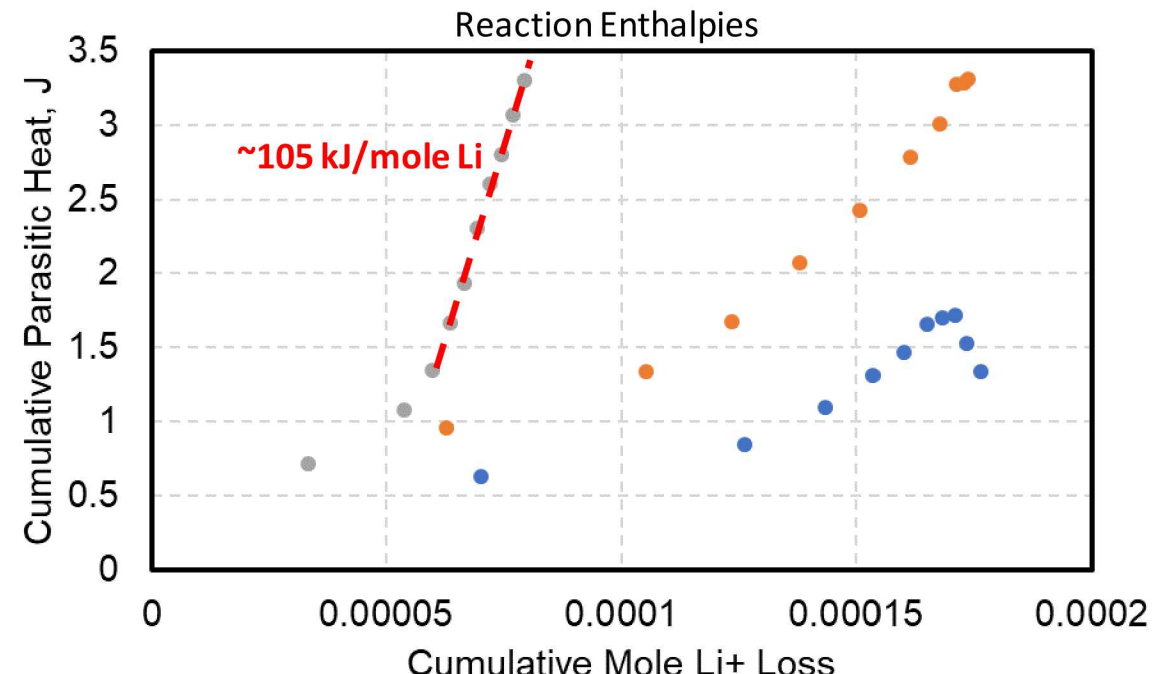


By calculating the accumulated parasitic heat flow per cycle, and plotting it against the accumulated irreversible capacity per cycle, we can observe the amount of parasitic heat for each mole of lithium lost

Mechanism of fade in both 50mV cells appears to be impedance-based, which does not correlate with parasitic heat flow

- Rising ohmic heat
- Fading total capacity usage
 - Cell capacity drops faster than accumulated irreversible capacity grows

Mechanism of fade in 100mV cell appears to be related to SEI growth and parasitic losses, stable ohmic behavior and linear fit curve after initial formation cycles



A. Tranchot, H. Idrissi, P.X. Thivel, L. Roue. *J. Power Sources* 330 (2016) 253.

Published dilatometry results show electrode growth become most sever below 100mV, in agreement with our observations

Shift of cycling window to 0.10 - 1.5V allows for avoidance of mechanical degradation in silicon and isolation of SEI passivation as mechanism of fade. Without mechanical losses, SEI reaction enthalpies can be calculated to be ~105 kJ/mole Li

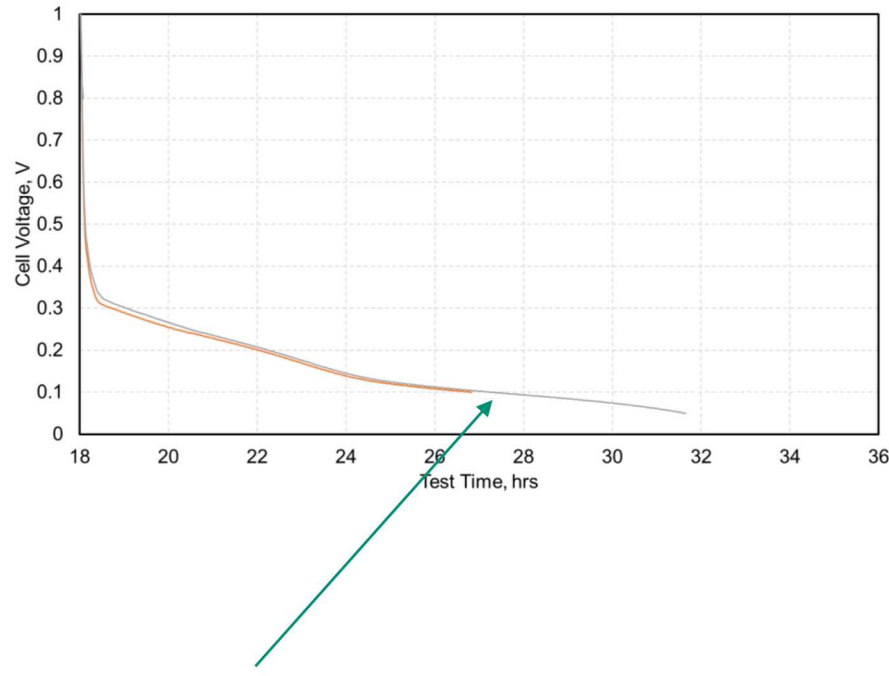
Similar approach showed higher reaction enthalpy (212 kJ/mol) for graphite, but lower heat flow and slower capacity fade

L.J. Krause, L.D. Jensen, J.R. Dahn. *J Electrochem Soc* 159 (2012) A937.

Cycle Life Comparison of Voltage Windows



C/10 Initial Lithiation Curve



100mV lower cutoff

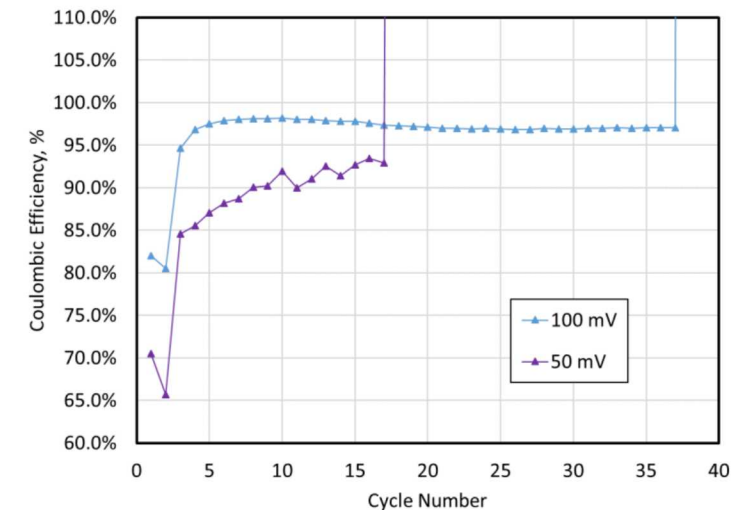
- First lithiation: 1850 mAh/g
- First delithiation: 1550 mAh/g

Roughly equivalent to $\text{Li}_{12}\text{Si}_7$ phase stoichiometry

Higher cutoff improves cycle life at the expense of initial capacity

Isolated passivation failure, which is still severe

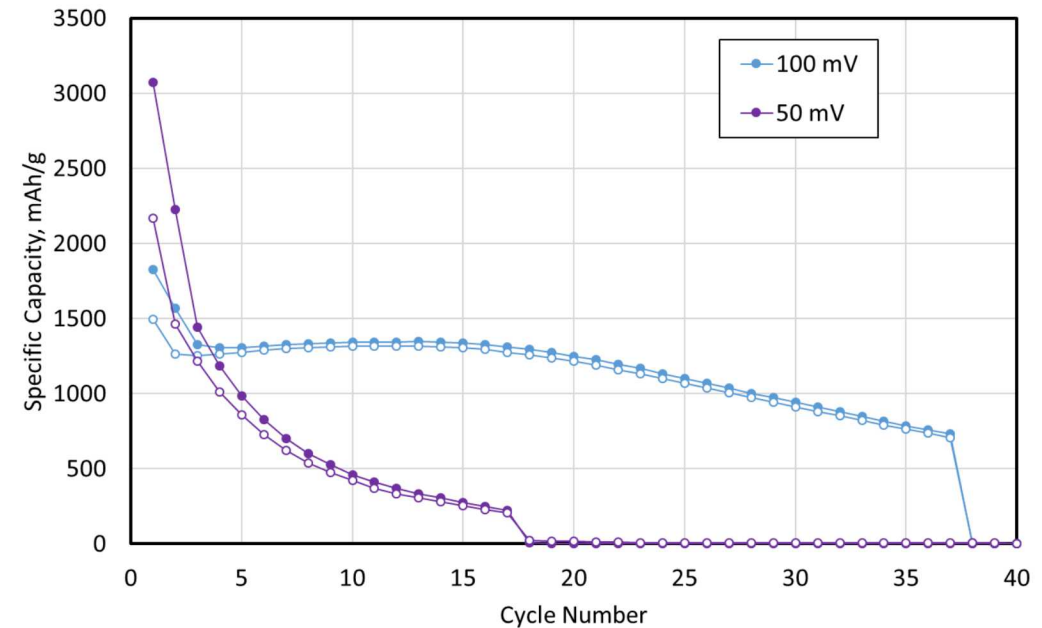
- Max CE = 98%
- Cell failure at cycle 37



50mV lower cutoff

- First lithiation: 3100 mAh/g
- First delithiation: 2200 mAh/g

Roughly equivalent to $\text{Li}_{13}\text{Si}_4$ phase stoichiometry





Operando Microcalorimetry of 80 wt.% nanoSi half cells

- Successful determination of Q-ohmic and Q-rev values enable accurate calculation of parasitic heat flow
- Variation in lower cutoff potential shows that lower voltage cycling (50mV) delivers higher capacity but results in more rapid capacity fade and cell failure due largely to mechanical pulverization and impedance effects
- Cycling at a higher cutoff voltage (100mV) delivers improvements in cycle life, but lower initial capacity. Also avoids mechanical degradation as primary means of capacity loss is correlated to SEI growth and parasitic heat flow
 - Able to be accurately characterized via *operando* microcalorimetry with a reaction enthalpy of 105 kJ/mol-lithium
 - SEI growth still causes severe cycling issues and failure before 40 cycles
- Parasitic heat flow associated with SEI growth shows stronger signal for lower C-rate, longer cycling times, indicating that the SEI is not passivating and continues to grow as a function of time

Acknowledgements



- Steven Trask and Bryant Polzin at the Argonne National Laboratory CAMP Facility for supplying the silicon electrodes used in this work.
- This work was supported by the US Department of Energy – Office of Energy Efficiency and Renewable Energy through the Vehicle Technology Office, program manager Brian Cunningham.
- Sandia National Laboratories is a multimission laboratory managed and operated by National Technology & Engineering Solutions of Sandia, LLC, a wholly owned subsidiary of Honeywell International Inc., for the U.S. Department of Energy's National Nuclear Security Administration under contract DE-NA0003525.



Backup Slides



Time Constant Determination and Dynamic Signal Correction (method)



The signal from the calorimeter is not indicative of the instantaneous heat generation within the calorimeter

- Measured signal is impacted by a combination of thermal transfer coefficients and specific heats
- Time constants can be determined to combine these factors and correct the measured signal
- Dependent upon inner configuration of calorimeter so measured using our coin cell fixture

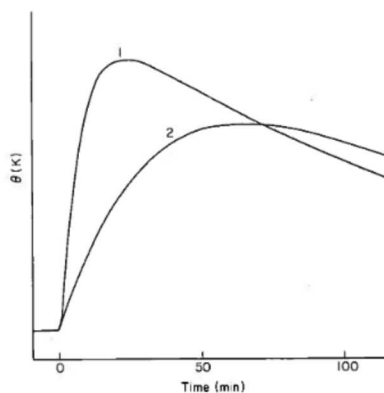


FIG. 2. Two thermograms representing the same process and obtained in the same calorimeter but with different inner heat exchange conditions.

$$q_x(t) = \alpha_{co} \left[\theta(t) + (\tau_1 + \tau_2) \frac{d\theta(t)}{dt} + \tau_1 \tau_2 \frac{d^2\theta(t)}{dt^2} \right]$$

TAM IV calorimeter can automatically calibrate static correction factors

$$q_{er} = \alpha_{co} \theta$$

$$q_x(t) = q_m(t) + (\tau_1 + \tau_2) \frac{dq_m(t)}{dt} + \tau_1 \tau_2 \frac{d^2q_m(t)}{dt^2}$$

Two time constants is typically enough to correct majority of signal discrepancy and can be easily determined experimentally based on known heat inputs

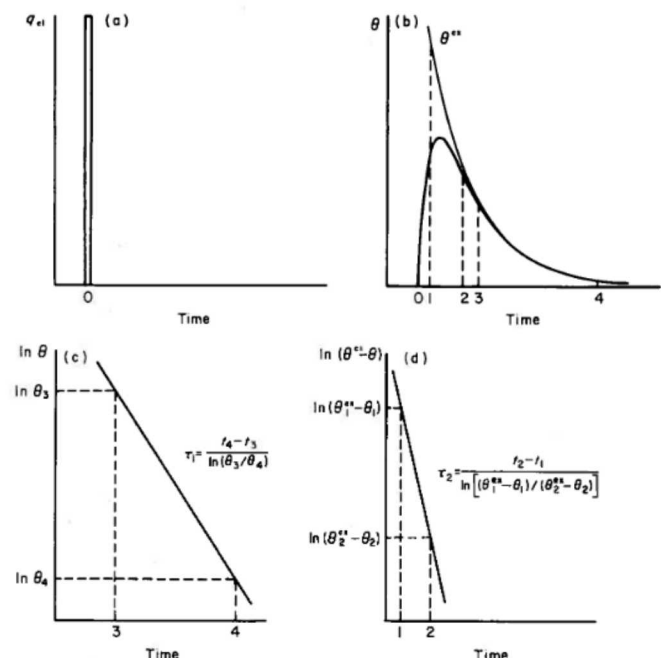


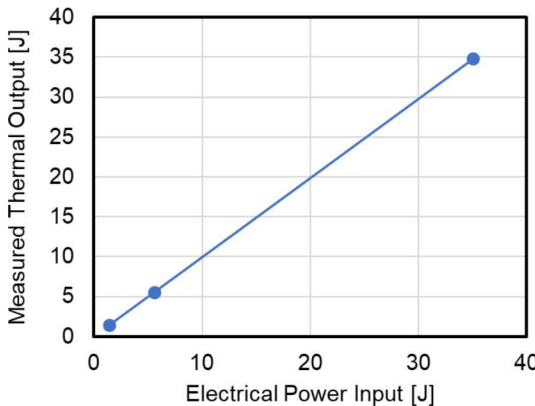
FIG. 3. Graphic presentation of the time-response procedure for determining time constants of the calorimeter.

Time Constant Determination and Dynamic Signal Correction (results)

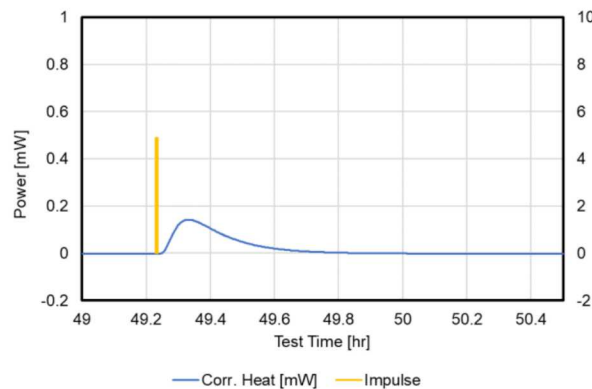


Assembled a “dummy” coin cell of known resistance and inserted into calorimeter coin cell fixture

- Enables controlled introduction of known heat in a coin cell form factor

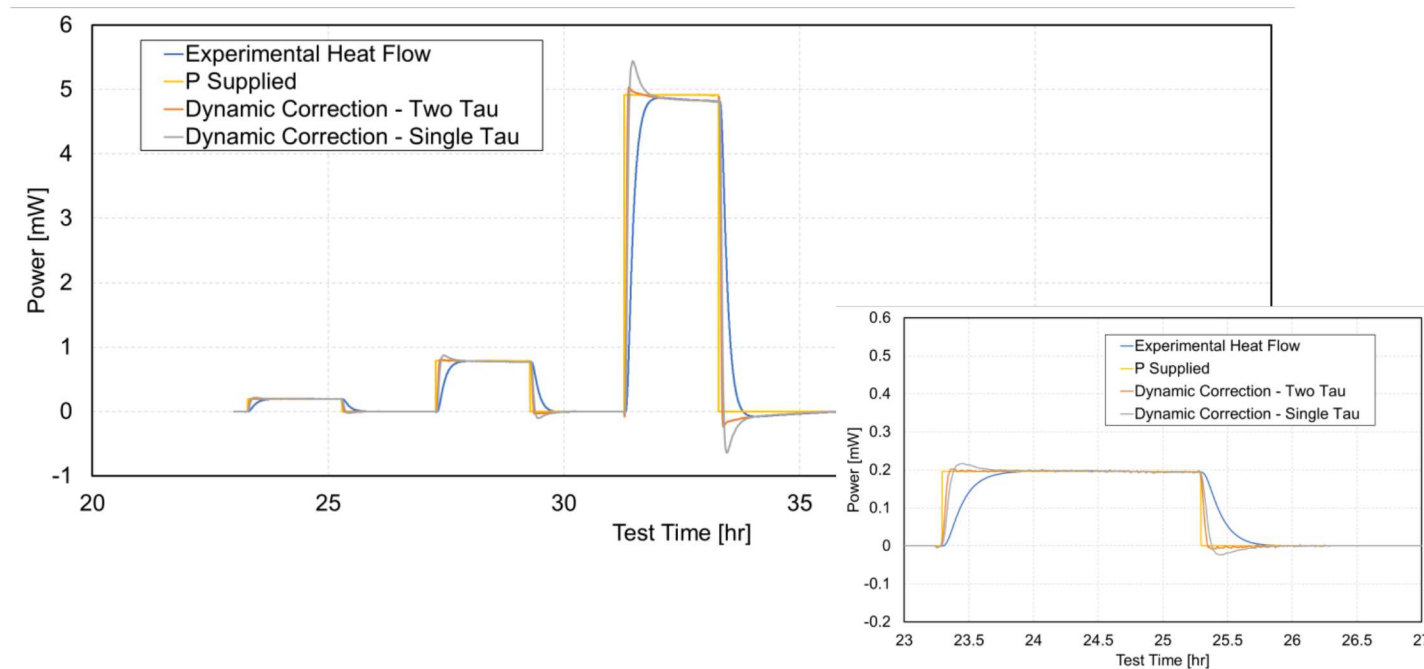


Static gain calibration is also confirmed here with total energy from each pulse measured within $\pm 0.5\%$



$$\tau_1 = 0.113 \text{ hrs} \approx 6 \text{ minutes}$$

$$\tau_2 = 0.034 \text{ hrs} \approx 2 \text{ minutes}$$



For raw signal it takes **28 minutes** to get the error below 2%
 For dynamically corrected signal, it takes **3 minutes**